Effect of Decorrelation on Butterfly Search Velocity Estimator Performance

Stephen A. McAleavey and Kevin J. Parker

Department of Electrical and Computer Engineering
University of Rochester, Rochester, NY 14627, USA

ABSTRACT

The effect of signal decorrelation on the performance of the Butterfly Search velocity estimator is examined. An analytical approximation for the expected value of the Butterfly Search $L(v)$ function is developed for three cases of interest. The approximations are verified against synthesized echo data. It is found that the peak value of the $L(v)$ function is limited by the rate of signal decorrelation. The performance of the Butterfly Search on synthesized data is calculated for varying SNRs and rates of decorrelation. The results show that improved performance may be obtained by processing and averaging subsets of echo ensembles, rather than applying the Butterfly Search to the entire ensemble simultaneously. For lower SNRs, processing the entire ensemble at once produces equivalent or better results than subset processing. Results from echo data obtained in-vitro are presented which confirm the simulations.

Keywords: Ultrasound, Doppler, Butterfly Search, decorrelation, noise, velocity estimation

1. INTRODUCTION

Color Doppler ultrasound is widely used for the clinical assessment of blood flow. Ultrasound techniques in general offer several advantages. They are non-invasive, the acoustical energy used is not harmful when appropriate power limitations are observed, images are produced in real time, and the associated equipment is relatively inexpensive.

Color Doppler systems provide a 2D map of blood velocity overlaid on a B-scan image. The signal processing method of Kasai et al.[1] and extensions to it are found in the great majority of Color Doppler systems.[2] The principle advantages of the Kasai method are its robustness and simplicity. Two shortcomings of the technique are often cited: reduced resolution compared to B-mode images produced with comparable equipment, and a limited range of distinguishable velocities. Several alternatives to Kasai processing have been proposed in the literature, including cross-correlation,[3] Wide-Band Maximum-Likelihood Estimation (WBMLE)[4] and Butterfly Search[5] methods. Each of these methods seeks to overcome both the limitations noted above.

The Butterfly Search finds the constant velocity which best describes the time shift among a group of echoes. This is in contrast to cross-correlation methods that calculate the time shift between pairs of echoes and compute a (possibly weighted) average of the results. One confounding issue for both techniques is that successive echoes may not be perfectly correlated for a number of reasons - noise, velocity shear, beam focus effects and lateral target movement, to name a few. Prior work by other researchers[6,7] has investigated the effect of echo to echo decorrelation on cross-correlation techniques. The goal of the present work is to determine the effect of echo decorrelation on the Butterfly Search and how best adapt the Butterfly Search to cope with the decorrelation.

1.1. The Butterfly Search

The Butterfly Search is described in detail in two papers[5,8] by Alam and Parker, and in Alam's Ph.D thesis.[9] The concept is, in short, to find the constant velocity which best explains the shift seen over an ensemble of echo signals or A-lines. The method is most easily explained by considering a point target case.

The received signal for a point target on the beam axis from the n^{th} transducer firing, $r_n(t)$, may be approximated as

$$r_n(t) = Gb(t - \tfrac{2d_0}{c} - \tfrac{2v}{c} n T_{PRF}) \quad 0 \le t \le T_{PRF} \tag{1}$$

Further author information: (Send correspondence to K.J.P)
S.A.M.: E-mail: mcaleave@ece.rochester.edu
K.J.P.: E-mail: parker@ece.rochester.edu

where $b(t)$ is the two-way transfer function of the transducer, G is a scale factor, d_0 the depth at $n = 0$, c the speed of sound and T_{PRF} the pulse repetition period ($T_{PRF} = \frac{1}{PRF}$). This model neglects beam diffraction effects and the Doppler frequency shift of the signal.

Equation 1's dependence on n is determined by the target velocity v. Any non-zero velocity results in a time shift of the echo signal between pulses. If the signal is sampled at constant delay $\frac{2d_0}{c}$ after each transducer burst, the received signal becomes a time-dilated version of the transmit signal, as described by Newhouse.[10] For a typical ultrasound system, which transmits a tone burst in Doppler mode, this means that the vector $r(\frac{2d_0}{c})$ describes a sampled, windowed sinusoid.

For $v = 0$, $r_n(t)$ is constant on n. If a time- varying delay $\frac{2\nu}{c} n T_{PRF}$ is introduced

$$r_n(t, \nu) = Gb(t - \frac{2d_0}{c} - \frac{2v}{c} n T_{PRF} + \frac{2\nu}{c} n T_{PRF}) \tag{2}$$

and ν is set equal to v, the same constant-on-n behavior is achieved. This is illustrated in Figure 1. If the value of ν for which $r_n(t, \nu)$ is constant can be found, then an estimate of velocity may be obtained.

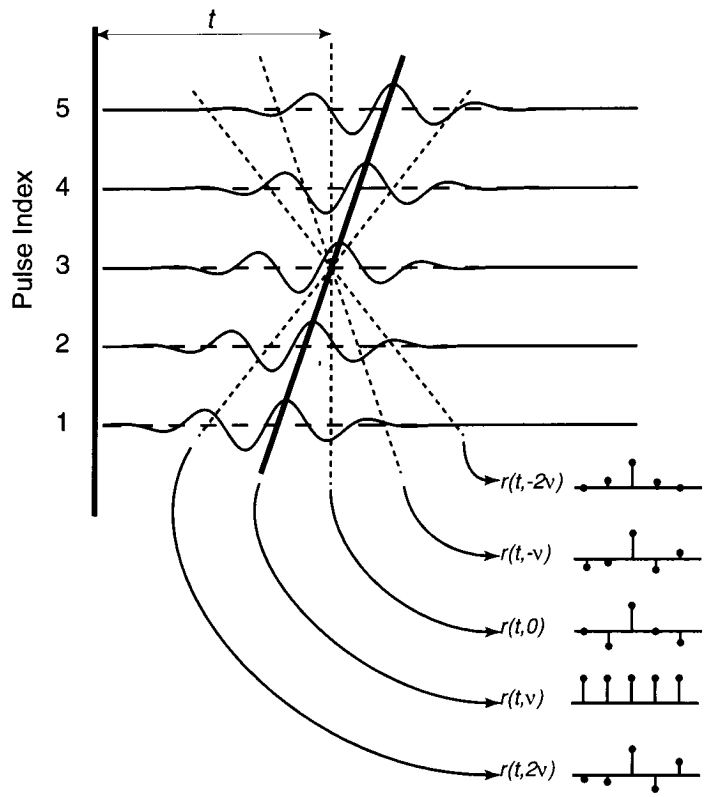

Figure 1. Butterfly Search signals for the ideal point-scatterer case.

A method for finding this constant value signal is provided in the $L(v)$ function of Alam and Parker.[5] The derivation of L begins with Schwartz's inequality:

$$\left| \sum_n g_1[n] g_2[n] \right|^2 \leq \sum_n |g_1[n]|^2 \sum_n |g_2[n]|^2 \tag{3}$$

where the equality is satisfied if and only if $g_1 = k g_2$.' Let g_1 be the re-sampled signal, and g_2 a constant value of 1. g_2 is then a scaled version of the resampled signal for $v = \nu$. Dividing both sides by the left hand g_1 summation yields

$$\frac{|\sum_n g_1[n] g_2[n]|^2}{\sum_n |g_1[n]|^2} \leq \sum_n |g_2[n]|^2 \tag{4}$$

Note that the left hand side is less than or equal to a constant. Since equality is achieved only when $g_1 = kg_2$, the left hand side will reach its peak only in the presence of a DC signal. Simplifying the above equation yields

$$\frac{\left|\sum_n g_1[n]\right|^2}{\sum_n |g_1[n]|^2} \leq N \tag{5}$$

Inserting the re-sampled signal $r_n(t,\nu)$ for g_1 finally gives the expression for $L(t,\nu)$

$$L(t,\nu) = \frac{\left|\sum_{n=0}^{N-1} r_n(t,\nu)\right|^2}{\sum_{n=0}^{N-1} |r_n(t,\nu)|^2} \tag{6}$$

This is the $L(v)$ function on RF of Alam and Parker, expanded as a function of time (depth). L takes on a maximum when $v = \nu$. Thus, the Butterfly Search involves calculating $L(\nu)$ for a range of ν and returning the ν which maximizes L as the estimate of velocity.

Since the amplitude of the RF signal varies sinusoidally with frequency f_0 while noise imposed on the signal from various sources will have a constant mean-square value, calculating $L(t,\nu)$ on the basis of the raw RF signal is likely to result in time-dependent performance, which is undesirable. This difficulty may be avoided by calculating $L(t,\nu)$ using either the analytic or quadrature representations of the RF signal. The analytic form may be found by calculating the Hilbert transform of the RF signal, which may be implemented as a FIR filter. Calculation of $L(t,\nu)$ with the analytic RF signal is precisely the same as with the real RF signal. With a quadrature signal, the matched filter is not a constant, but a complex sinusoid on n whose frequency depends on ν. Separate matched filters must be calculated for each value of ν and applied in calculating $L(t,\nu)$ with quadrature signals. In either case, the cyclicly varying performance problem is eliminated.

Although velocity resolution improves with the number of A-lines, several factors limit the number of A-lines that may be used in the velocity estimate. Decorrelation of the echoes, due to lateral movement through the beam and/or velocity gradient effects, is one limitation. Another is the spread of axial ranges included in an estimate, which increases linearly with the number of A-lines used. For any non-zero beam-vessel angle, this can result in the collection of data from targets with velocities significantly different from that of the central point. These effects suggest that a small number of pulses could be expected to yield the best Butterfly estimate.

2. THEORY

2.1. Signal

Consider now the case illustrated in Figure 2. A cloud of independently distributed, sub-resolvable scatterers passes through the ultrasound beam. The scatterers have axial velocity v_x and lateral velocity v_y. The successive echo signals can no longer be assumed to be identical but for a time shift. Rather, the similarity between echo signals depends on the lateral velocity and the lateral pulse width. If $v_y = 0$, then successive pulses will differ only in time delay. Likewise, low lateral velocities and wide pulses suggest greater correlation between successive pulses than high lateral velocities and narrow pulses.

In this situation the resampled signals r are more meaningfully handled as random vectors than deterministic functions of the pulse and scatterer positions. The statistics of any particular r will depend on the pulse shape, axial and lateral velocity. Let us define a random vector $\mathbf{Z}$ representing any particular $r(t,\nu)$,

$$\mathbf{Z} = [z_1, z_2, \ldots, z_n] = [\hat{r}_1(t,\nu), \hat{r}_2(t,\nu), \ldots, \hat{r}_n(t,\nu)] \tag{7}$$

where the $\hat{r}_i(t,\nu)$ are complex valued samples obtained from the Hilbert-transformed echo signals. $\mathbf{Z}$ is a vector of correlated complex random variables with a Gaussian distribution,[11] taken from the ensemble of echo signals. The probability density function of $\mathbf{Z}$ is

$$f_{\mathbf{Z}}(Z) = \frac{1}{\pi^n C_{ZZ}} \exp(ZC_{ZZ}^{-1}(Z^T)^*) \tag{8}$$

$\mathbf{Z}$ is defined completely by the correlation matrix C_{ZZ}. The values of the matrix C_{ZZ} will in general depend on τ, v_x, v_y, and on the pulse characteristics.

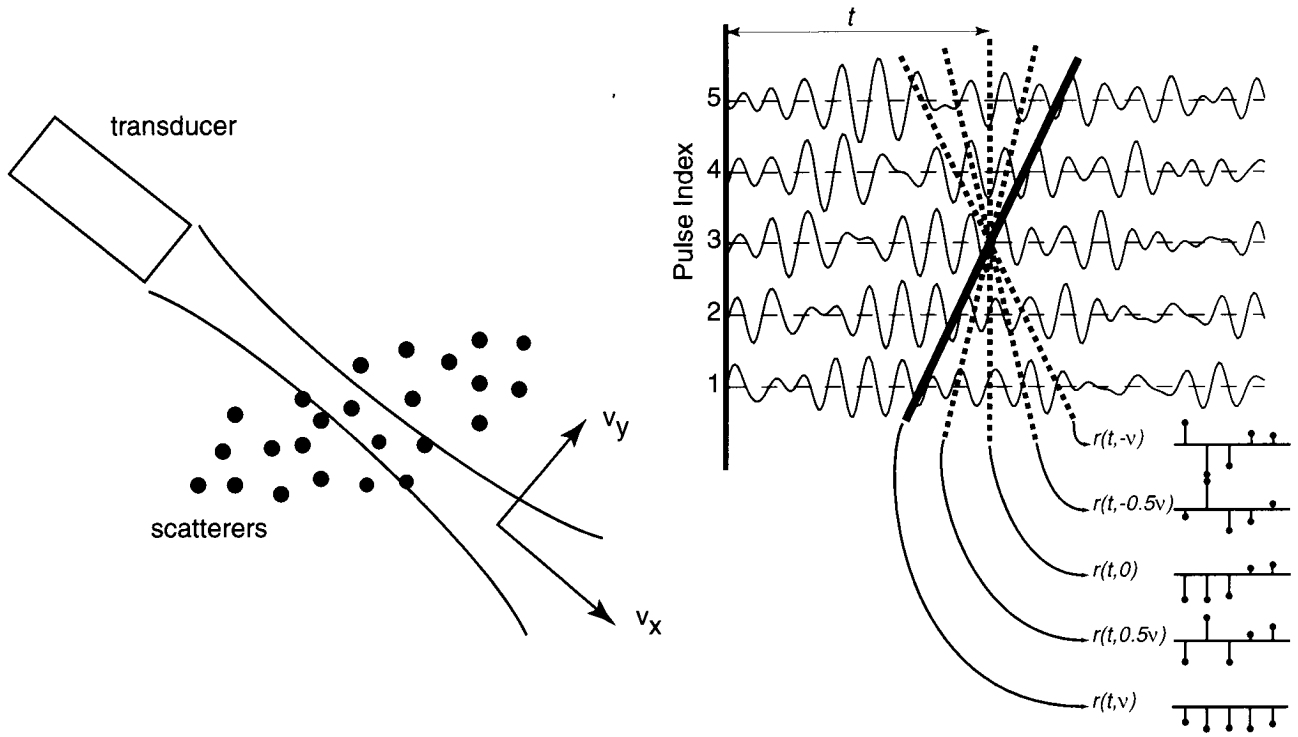

Figure 2. Physical setup and flow signals for 2D velocity case.

2.1.1. Expected value of L

From the definition of the expected value of a function of a random variable,[12] the mean value of $L(t,\nu)$ is*

$$E\{L\} = 1 + \int_{-\infty}^{\infty} \cdots \int_{-\infty}^{\infty} \frac{\sum_{i=1}^{n-1} \sum_{j=i+1}^{n} (z_i^* z_j + z_i z_j^*)}{\sum_{k=1}^{n} |z_k^2|} \frac{1}{\pi^n C_{ZZ}} exp(ZC_{ZZ}^{-1} Z^+) dz_1 \ldots dz_n \tag{9}$$

Evaluation of the expected value is difficult in general because the elements of $\mathbf{Z}$ may be correlated. A numerical integration might, after considerable computation, yield an answer, but this would provide little insight. However, three specific cases of interest can be approximated. These are the cases of short pulses, uncorrelated additive noise, and phase decorrelation.

Short Pulses (Uncorrelated Samples) In this case, the z_i are uncorrelated. This occurs when

$$\frac{|\nu - v|}{2c} T_{prf} > T_{pulse} \tag{10}$$

that is, the magnitude of difference between the target velocity and the velocity corresponding to the butterfly line being calculated is great enough that the pulses do not lie in overlapping regions of tissue. Therefore, the samples are independent. The resulting samples are uncorrelated, zero mean Gaussian distributed.[11] The uncorrelated condition is sufficient to calculate the expectation for L in such a case,

$$E\{L\} = E\left\{1 + \frac{2\sum_{i=1}^{n-1} \sum_{j=i+1}^{n} (z_i^* z_j + z_i z_j^*)}{\sum_{k=1}^{n} |z_k|^2}\right\} = 1. \tag{11}$$

since $E(z_i^* z_j) = E(z_i z_j^*) = 0$ for $i \neq j$.

*Note that $|\sum_{i=1}^{n} z_i|^2 / \sum_{j=1}^{n} |z_j|^2 = 1 + \sum_{i=1}^{n-1} \sum_{j=i+1}^{n} (z_i z_j^* + z_i^* z_j) / \sum_{k=1}^{n} |z_k|^2$

Uncorrelated Noise The next degree of complexity involves a constant signal in the presence of noise. In this case, the random vector $\mathbf{Z}$ is described by

$$\mathbf{Z} = [\ a + \varsigma_1 \quad a + \varsigma_2 \quad \ldots \quad a + \varsigma_n\ ] \tag{12}$$

where a is a real constant, and $\varsigma_i = x_i + jy_i$, where x and y are independent Gaussian random variables, with zero mean and variance σ^2, representing additive noise. The expression for the expected value of L my be written

$$E\{L\} = 1 + \sum_{j=1}^{n-1} \sum_{i=j+1}^{n} \left(E\left\{ \frac{2a^2}{\sum_{k=1}^{n} |z_k|^2} \right\} + E\left\{ \frac{a\varsigma_i + a\varsigma_i^*}{\sum_{k=1}^{n} |z_k|^2} \right\} + E\left\{ \frac{a\varsigma_j + a\varsigma_j^*}{\sum_{k=1}^{n} |z_k|^2} \right\} + \left\{ \frac{\varsigma_i^* \varsigma_j + \varsigma_i \varsigma_j^*}{\sum_{k=1}^{n} |z_k|^2} \right\} \right) \tag{13}$$

The last three expectations in the double sum can be approximated as zero. Thus we are left with the simplified expression

$$E\{L\} = 1 + 2a^2 \sum_{i=1}^{n-1} \sum_{i=j+1}^{n} \left(E\left\{ \frac{1}{\sum_{k=1}^{n} |z_k|^2} \right\} \right). \tag{14}$$

The modified Rician probability density function of z_k was found by Goodman.[13] Using the central limit theorem the random variable described by the summation in the denominator may be approximated as Gaussian with a mean of $n(2\sigma^2 + a^2)$ and variance of $4n\sigma^4(1 + \frac{a^2}{\sigma^2})$. Using the method of approximation by moments,[12] a first-order estimate of the expected value is given by

$$E\{L\} = 1 + \frac{(n-1)a^2}{a^2 + 2\sigma^2} \tag{15}$$

noting that $\sum_{i=1}^{n-1} \sum_{j=i+1}^{n} 1 = \sum_{i=1}^{n-1} n = \frac{n^2 - n}{2}$. This approximation is plotted in Figure 3 for a range of values of the ratio a/σ, along with mean values of L for ensembles of 10^4 computer-generated random vectors with the specified values of a and σ.

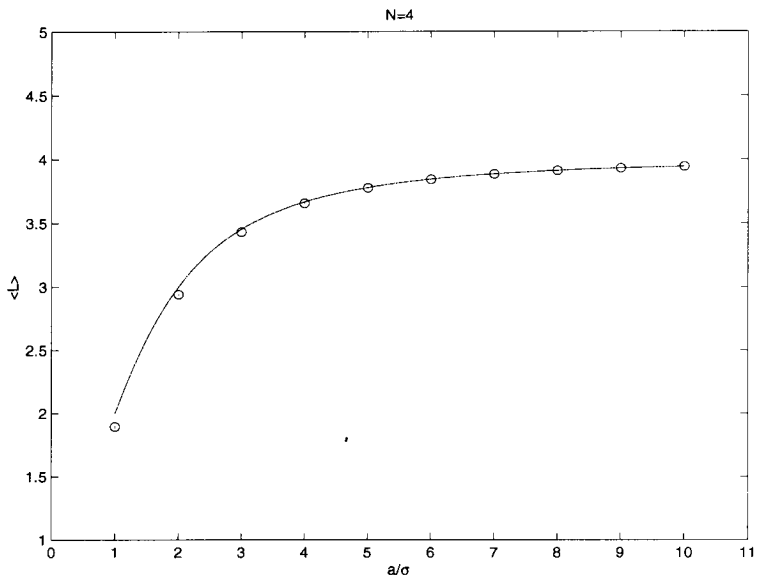

Figure 3. Expected value of L as a function of $\frac{a}{\sigma}$ with $n = 4$. o's denote mean estimated from an ensemble of 10^4 random vectors.

Correlated Z For the general case where the elements of $\mathbf{Z}$ are correlated calculation of the expected value becomes more difficult. We define $\mathbf{Z}$ as

$$\mathbf{Z} = [\mathbf{z}_1 + \varsigma_1, \mathbf{z}_2 + \varsigma_2, \ldots, \mathbf{z}_n + \varsigma_n] \tag{16}$$

with ς_i as described above. The $\mathbf{z}_i$ are correlated complex Gaussian random variables with correlation matrix C_{zz}.

The expression for the expected value is then

$$E\{L\} = 1 + \sum\sum \left(E\left\{ \frac{z_i^* z_j + z_i z_j^*}{\sum_k |z_k|^2} \right\} + E\left\{ \frac{z_i^* \varsigma_j + z_i \varsigma_j^*}{\sum_k |z_k|^2} \right\} + E\left\{ \frac{z_j^* \varsigma_i + z_j \varsigma_i^*}{\sum_k |z_k|^2} \right\} + E\left\{ \frac{\varsigma_i^* \varsigma_j + \varsigma_i \varsigma_j^*}{\sum_k |z_k|^2} \right\} \right) \quad (17)$$

The last three expected values can be taken to be zero. The leftmost expectation presents a problem in that the numerator and denominator terms are not independent. In order to attempt an analytical approximation, the denominator will be replaced by a constant, determined as in the uncorrelated noise case above. This accurately models the case where the elements of $\mathbf{Z}$ differ only in phase. It also provides a fair approximation for slowly varying envelope amplitude, as will be shown below. We will show that for even small values of n this is a fair approximation. Thus simplified, the expression may be rewritten as

$$E\{L\} = 1 + \frac{2}{n(a^2 + 2\sigma^2)} \sum_{i=1}^{n-1} \sum_{j=i+1}^{n} \Re(E\{z_i z_j^*\}) \quad (18)$$

where $\Re(\xi)$ is the real part of ξ. With this expression arrived at, it is possible to determine how the expected value of L behaves as a function of n, given a correlation matrix C. A case of particular interest is that in which the butterfly line being estimated represents the correct axial target velocity, while a lateral flow component results in decreasing correlation with increasing temporal separation of pulses. It is reasonable to expect that the elements of the correlation matrix C_{ij} depend only on the difference $j - i$, and that $\Re(C_{ij}) = f(j - i)$. This allows the double summation to be reduced to a single sum

$$E\{L\} = 1 + \frac{2}{n(a^2 + 2\sigma^2)} \sum_{i=1}^{n-1} if(n - i) \quad (19)$$

A simple but plausible model for the correlation between pulses[6] is given by

$$\Re(C_{ij}) = \Re(E\{z_i z_j^*\}) = \begin{cases} \frac{a^2(b - |i-j|)}{b} & |\, i - j \,| \leq b \\ 0 & \text{otherwise} \end{cases} \quad (20)$$

After substituting into the expression for $E\{L\}$ and performing some tedious algebra we arrive at

$$E\{L\} = \begin{cases} \frac{a^2(-n^2+3bn-3b+1)}{3b(a^2+2\sigma^2)} & n \leq b+1 \\ \frac{a^2}{(a^2+2\sigma^2)}\left(b - 1 - \frac{b^2-1}{3n}\right) & n > b+1 \end{cases} \quad (21)$$

The expected value of L is described by a quadratic for $n \leq b + 1$, while for $n > b + 1$ the expected value slowly increases from the $n = b + 1$ value and reaches a limit of $\frac{a^2(b-1)}{a^2+\sigma^2}$ as $n \to \infty$. The expected value of L as a function of n is plotted in Figure 4 for several values of b and σ to illustrate the general behavior of the function.

This expression suggests how best to process a collection of RF samples with the Butterfly Search. When the correlation between RF samples is high over all n samples, that is, when $b \gg n$, $E\{L\}$ increases steadily with n. The expected value of L does not increase substantially for $n > b$. Therefore, there is no benefit in using more than about b pulses in the Butterfly calculation. This is not to say that more than b pulses are not helpful. If additional pulses are available, they may still be put to good use by splitting the data into sets. Suppose $2b$ pulses are available for processing. A single Butterfly over the $2b$ pulses is little better than a Butterfly over b pulses. However, 2 Butterflies of b pulses may be averaged, with a consequent halving of the variance of L. This improves the probability that the correct velocity is selected. This idea is illustrated in Figure 8, where the analytical approximation for $E(L)$ for the case of correlated samples is compared with the ensemble results from the data generated in the next section. Notice that when using 16 A-lines, splitting the data into smaller sets produces a greater expected value for L than processing all 16 A-lines in a single Butterfly, as predicted by the approximation.

3. SIMULATION

The expressions developed in the previous section for the expected value of $L(t, \nu)$ are helpful in predicting the behavior of the Butterfly Search under conditions of signal decorrelation and noise, but they do not provide the

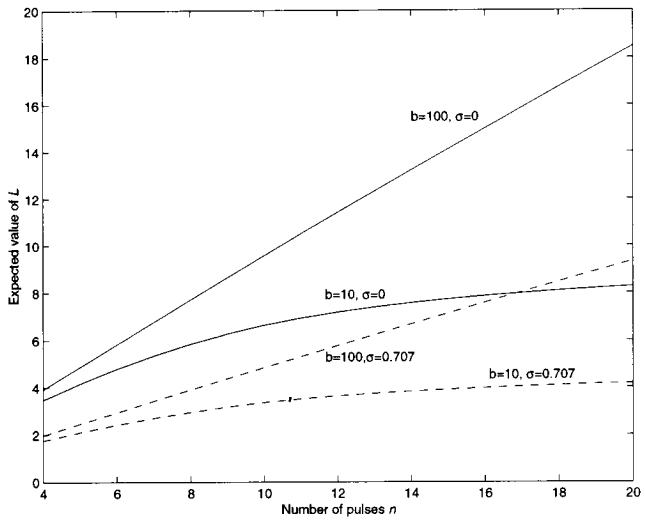

Figure 4. Expected value of L as a function of n. $a = 1$ for all traces.

complete picture. To estimate the performance of the Butterfly Search under these conditions, a simulation study was carried out. Synthetic echo signals were generated with specific axial and lateral velocity and noise components. The Butterfly Search was then used to estimate the axial velocity described by these signals. The use of synthetic echo signals allowed the performance of the Butterfly Search to be estimated over a wide range of decorrelation and noise conditions. Performance was gauged relative to Signal to Noise Ratio (SNR), number of A-lines used in the estimate, lateral velocity, and processing technique.

To generate the simulated echo signals, an 8192x512 array of Gaussian-distributed random variates was created. The spatial sampling frequency was fixed at 100μm, and 1-D Gaussian-enveloped sinusoidal pulses ($f_0 = 7.5$MHz, $\sigma_{\text{axial}} = 0.13$mm) were generated. The pulses were convolved with the 512 columns of the scatterer array to generate RF signals. The contribution of each column to the final RF signal was weighted by the lateral beam profile (Gaussian, $\sigma = 0.2$mm) and summed to generate a single RF A-line. The process was repeated, using the same scatterer array, with the lateral profile shifted by an amount determined by the lateral flow velocity for the particular simulation, ranging between 0 and 0.5m/s. 50 A-lines were generated in each case. No stationary clutter or wall filtering was simulated. Though wall filtering would be needed in a practical system, these simulations are concerned solely with the performance of the Butterfly Search under conditions of signal decorrelation and additive noise.

The performance for each rate of decorrelation as a function of the number of A-lines used in the Butterfly calculation was found. The velocity was estimated at 600 points in each data set. The $L(t, \nu)$ function was calculated for $-77 \leq \nu \leq 77$cm/s. Note that this velocity range is greater than can be achieved with the Kasai-autocorrelation method ($\pm$25cm/s), which is limited by sampling frequency considerations. The ν were quantized in steps of 0.77cm/s. Velocity estimates were calculated with odd integer numbers of A-lines, from 3 to 21, and the fraction of velocity estimates within ± 3 bins, i.e. $\pm$2.3cm/s, stored. The results are plotted in Figures 5-7. It can be seen from the figures that while using more A-lines in the calculation always produces a superior result, the sensitivity of the result to the number of A-lines used increases with decreasing SNR.

To determine if averaging several smaller butterflies would produce better results than a single large butterfly, a second simulation was performed. Using the same simulated echo data sets and velocity range as above, the butterfly velocity estimate was calculated with 16 A-lines, using three different methods. The first was a straightforward calculation using 16 A-lines in one large butterfly. The second used the average of the $L(t, \nu)$ of two butterflies of 8 A-lines each. The third used the average of the $L(t, \nu)$ of 4 butterflies of 4 A-lines each. In all cases, the maximum of the resulting $L(t, \nu)$ was selected as the velocity estimate. The results are compiled in Table 1.

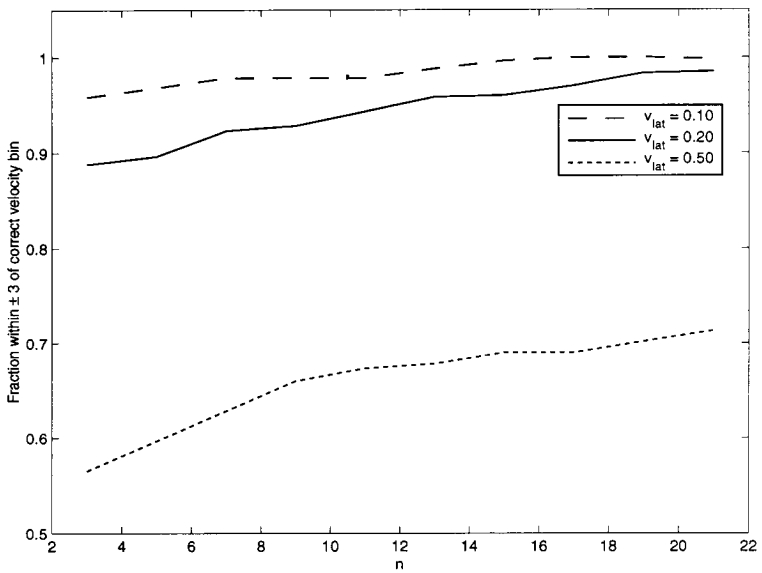

Figure 5. Fraction of velocity estimates within ±3 velocity bins for lateral velocities of 0.1, 0.2 and 0.5 m/s, SNR $= \infty$

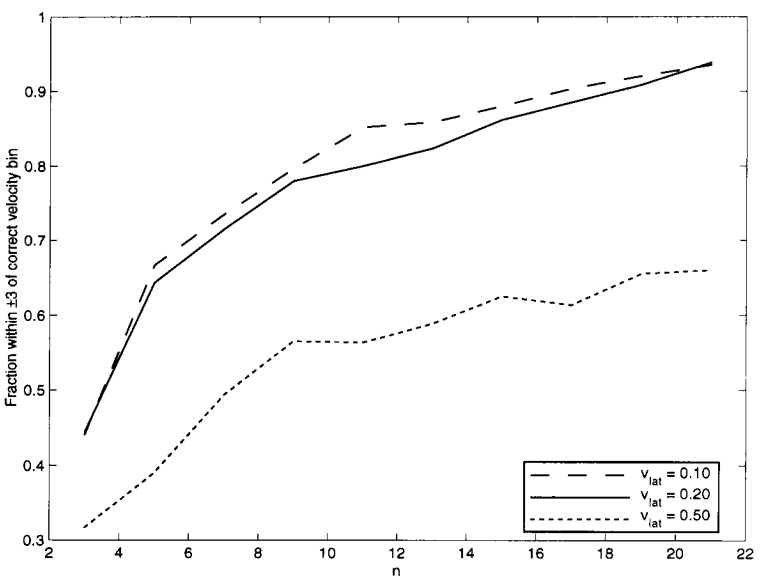

Figure 6. Fraction of velocity estimates within ±3 velocity bins for lateral velocities of 0.1, 0.2 and 0.5 m/s, SNR = 6dB.

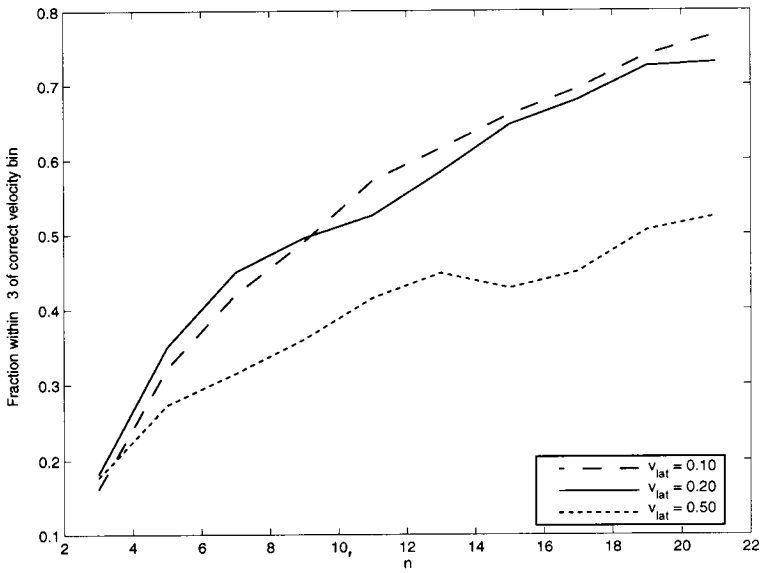

Figure 7. Fraction of velocity estimates within ± 3 velocity bins for lateral velocities of 0.1, 0.2 and 0.5 m/s, SNR = 0dB.

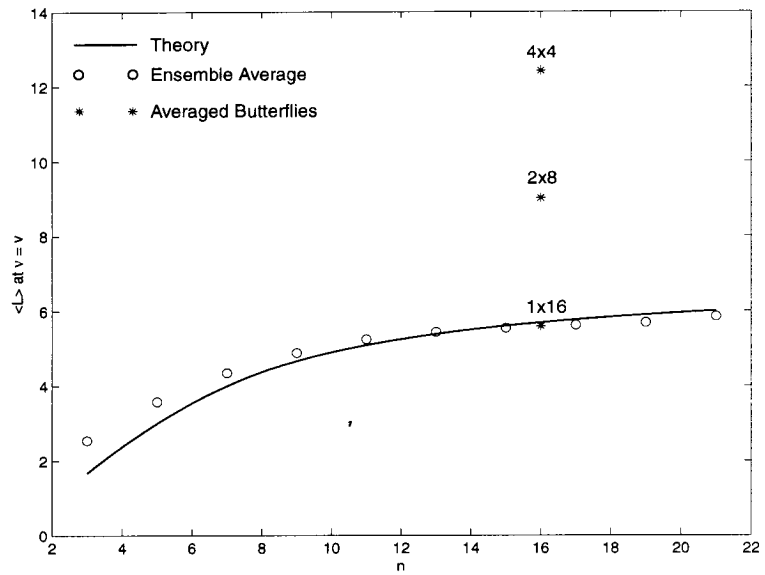

Figure 8. Expected value of L as a function of n. $v_{\text{lateral}} = 0.5$m/s. Solid curve denotes analytic estimate for b=8. Circles denote ensemble average results with a Gaussian windowed pulse. Stars represent the ensemble average results for one butterfly of 16 A-lines (1x16), 2 butterflies of 8 A-lines (2:8) and 4 butterflies of 4 A-lines.

Table 1. Fraction of estimates within ±3 velocity bins of correct value. n=16. x:y indicates x Butterflies of y A-lines.

SNR = ∞

	v_{lateral}(m/s)						
	0.00	0.01	0.02	0.05	0.10	0.20	0.50
1:16	1.00	1.00	1.00	1.00	1.00	0.96	0.69
2:8	1.00	1.00	1.00	1.00	1.00	0.97	0.72
4:4	1.00	1.00	1.00	1.00	1.00	1.00	0.86

SNR = 6dB

	v_{lateral}(m/s)						
	0.00	0.01	0.02	0.05	0.10	0.20	0.50
1:16	0.88	0.89	0.90	0.90	0.89	0.88	0.63
2:8	0.81	0.84	0.84	0.82	0.83	0.87	0.63
4:4	0.72	0.73	0.72	0.73	0.76	0.82	0.71

SNR = 0dB

	v_{lateral}(m/s)						
	0.00	0.01	0.02	0.05	0.10	0.20	0.50
1:16	0.69	0.71	0.70	0.69	0.68	0.67	0.42
2:8	0.58	0.61	0.63	0.60	0.59	0.64	0.44
4:4	0.45	0.46	0.48	0.47	0.45	0.54	0.41

4. EXPERIMENT

As a further check of the analysis presented here, a water-tank experiment was performed. Ultrasound echoes from a moving target were acquired with a commercial medical scanner (HP Sonos-100), which has been modified to provide RF output and timing signals. The mechanically-steered transducer used had a center frequency of 2.5MHz. The target consisted of a block of tissue-mimicking material, attached to a linear translation stage. The computer-controlled stage allows for movement of the block in 2.5μm steps. The ultrasound transducer was mounted on a gimbal such that the angle between the ultrasound beam and the linear stage could be varied over a range of 0–60 degrees in 15 degree increments. The transducer to target distance was arranged to keep the target at or beyond the focus of the ultrasound beam. 160 echo signals were generated for each angle, with a translation of 75 microns occurring between each echo. The RF signals were captured with a digital oscilloscope (LeCroy 9430) and transfered to disk for later processing. The SNR was in excess of 20dB.

Figure 9 illustrates the results of two Butterfly processing techniques on the water-tank data. The first method was to compute the Butterfly estimate based on a single L calculation using 16 A-lines. The second was to average 4 L calculations, each with 4 A-lines. To emphasize the effect of decorrelation, the A-line data was subsampled in pulse index, resulting in a translation of 225μm between A-lines. For a 5kHz pulse repetition frequency, this is equivalent to a target velocity of 1.1m/s. The data points presented in Figure 9 represent the average of 400 trials. As in the computer simulations, the average of smaller Butterflies performs better than a single large Butterfly in the presence of signal decorrelation, when the SNR is high.

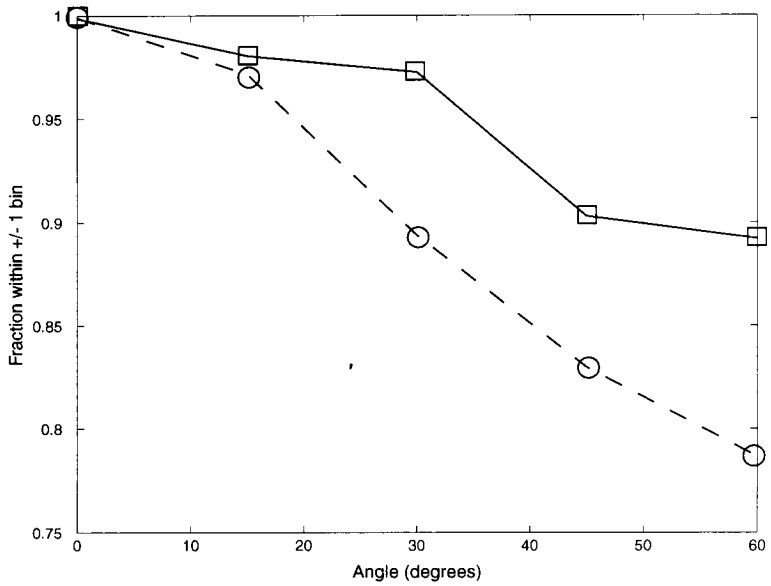

Figure 9. Performance of Butterfly estimator on water tank data versus angle. Circles denote data points for calculation using a one Butterfly of 16 A-lines. Squares indicate results for the average of four Butterflies of four A-lines each..

5. CONCLUSION

The effect of echo-to-echo decorrelation on Butterfly Search estimation has been assessed. An analytical approximation to the expected value of the L function has been found for several cases of interest, and all are found to be in good agreement with results obtained by ensemble averaging. The approximations indicate that the maximum value of the L function is limited by the rate of signal decorrelation. Simulations show that this correlates well with the performance achieved by the Butterfly Search on decorrelated data. Finally, it is found that by processing echo ensembles in subsets and averaging the results, superior performance may be achieved compared to that obtained by processing the echo ensemble in one Butterfly. This performance improvement is limited by the SNR of the echo ensemble. Future work may investigate methods for automatically selecting the optimum Butterfly processing technique, based on the signals to be processed.

REFERENCES

1. C. Kasai, K. Namekawa, A. Koyano, and R. Omoto, "Real-time two-dimensional blood flow imaging using an autocorrelation technique," *IEEE Transactions on Sonics and Ultrasonics* **SU-32**, pp. 458–464, May 1985.
2. J. A. Jensen, *Estimation of Blood Velocities Using Ultrasound: A Signal Processing Approach*, Cambridge University Press, 1996.
3. O. Bonnefous and P. Pesqué, "Time domain formulation of pulse-Doppler ultrasound and blood velocity estimation by cross correlation," *Ultrasonic Imaging* **8**, pp. 73–85, 1986.
4. K. W. Ferrara and V. R. Algazi, "A new wideband spread target maximum likelihood estimator for blood velocity estimation—Part I: Theory," *IEEE Transactions on Ultrasonics, Ferroelectronics and Frequency Control* **38**, pp. 1–16, January 1991.
5. S. Alam and K. Parker, "The butterfly search technique for estimation of blood velocity," *Ultrasound in Medicine and Biology* **21**(5), pp. 657–70, 1995.
6. S. G. Foster, P. M. Embree, and W. D. O'Brien, Jr., "Flow velocity profile via time-domain correlation: Error analysis and computer simulation," *IEEE Transactions on Ultrasonics, Ferroelectronics and Frequency Control* **37**, pp. 164–175, May 1990.
7. P. M. Embree and W. D. O'Brien, Jr., "Volumentric blood flow via time-domain correlation: Experimental verification," *IEEE Transactions on Ultrasonics, Ferroelectronics and Frequency Control* **37**, pp. 176–189, May 1990.

8. S. Alam and K. Parker, "Reduction of computational complexity in the butterfly search technique ultrasonic blood flow imaging," *IEEE Transactions on Biomedical Engineering* **43**, pp. 723–733, July 1996.
9. S. K. Alam, *The Butterfly Search Velocity Estimation Technique for Doppler Ultrasound Flow Imaging.* PhD thesis, University of Rochester, Department of Electrical Engineering, April 1996.
10. V. Newhouse and I. Amir, "Time dilation and inversion properties and the output spectrum of pulsed Doppler flowmeters," *IEEE Transactions on Sonics and Ultrasonics* **30**, pp. 174–179, May 1983.
11. R. W. Wagner, M. F. Insana, and D. G. Brown, "Statistical properties of radio-frequency and envelope-detected signals with application to medical ultrasound," *Journal of the Optical Society of America A* **4**, pp. 910–922, May 1987.
12. A. Papoulis, *Probability, Random Variables and Stochastic Processes*, McGraw-Hill, Inc., third ed., 1991.
13. J. Goodman, "Statistical properties of laser speckle patterns," in *Laser Speckle and Related Phenomena*, J. Dainty, ed., ch. 2, Springer-Verlag, Berlin, 1975.